Electronic Supplementary Information(ESI)

Noble-metal-free Single-phase $Co_3V_2O_8$ with Structural Integrity of Nanofibers for Selective Detection of Ascorbic Acid

Dasol Jin[1], Song Hee Lee[1], Youngmi Lee*, Chongmok Lee* and Myung Hwa Kim*

Department of Chemistry & Nanoscience, Ewha Womans University, Seoul 03760, Korea.

* Corresponding authors

E-mail: youngmilee@ewha.ac.kr; cmlee@ewha.ac.kr; myungkim@ewha.ac.kr

[1]Authors contributed equally to this work.

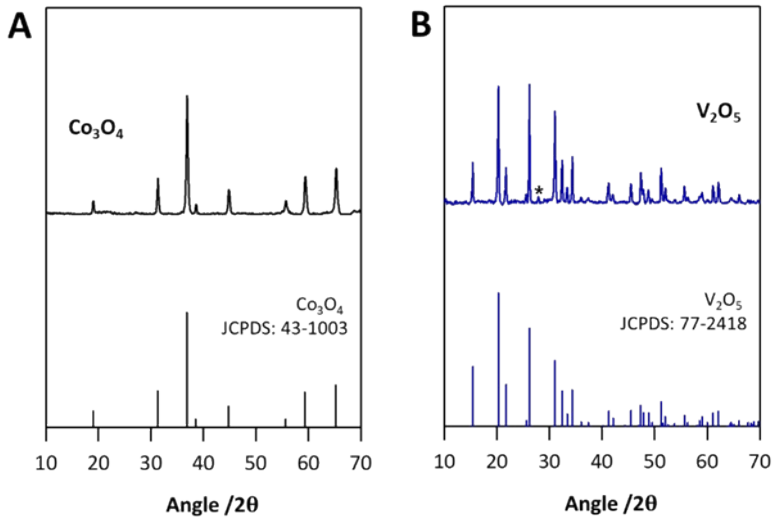

Fig. S1. XRD patterns of (A) Co_3O_4 and (B) V_2O_5 with JCPDS references. The peak marked with * corresponds with VO_2.

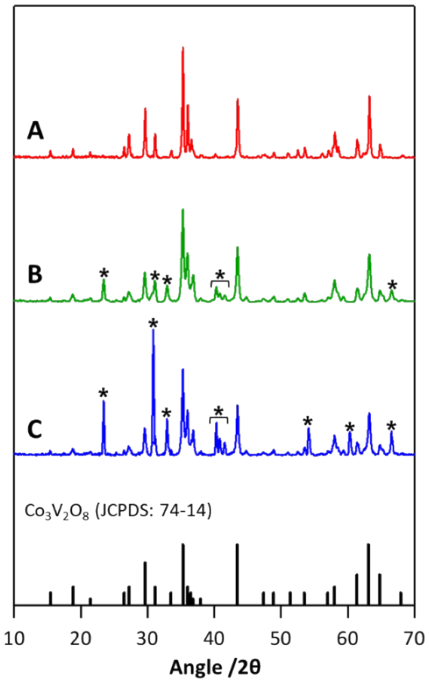

Fig. S2. XRD patterns of as-prepared Co/V mixed oxides after being thermally calcined for 1 h at various annealing temperatures of (A) 500 °C, (B) 650 °C and (C) 800 °C, respectively. The peaks marked with * correspond with CoV_2O_6.

The XRD patterns of Co/V mixed oxides thermally annealed at different temperatures are presented in Fig. S2. For all samples, major diffraction peaks were consistent with the cubic crystal structure of $Co_3V_2O_8$ (JCPDS: 74-14). However, increase in annealing temperature led to phase separation; the Co/V mixed oxide system prepared at 800 °C (Fig. S2-C) was eventually phase-separated into $Co_3V_2O_8$ and CoV_2O_6, respectively. Therefore, we extrapolate that thermoresponsive phase behavior of the Co/V mixed oxide can be attributed to an oxidation-state-dependent lattice formation.

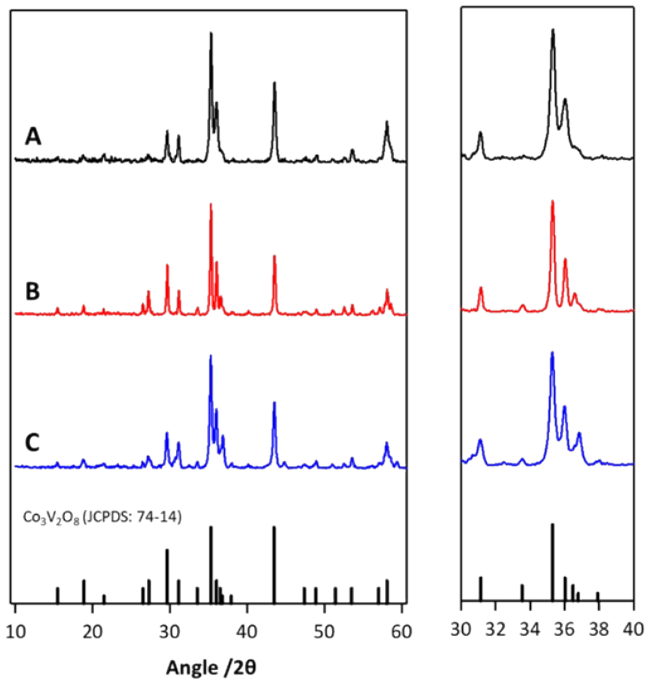

Fig. S3. XRD patterns of as-prepared Co/V mixed oxides after being thermally annealed at 500 °C with (A-C) different retention times: (A) 20 min, (B) 60 min and (C) 180 min. Note that the XRD patterns (right side) are expanded diffraction peaks of prepared samples with 2θ ranging from 30°–40° as a function of *x*.

In sharp contrast to the phase formation of Co/V mixed oxides series with different annealing temperatures, a series of nanomaterials, thermally annealed at a fixed temperature of 500 °C but for various retention times (*t*), exhibited distinct peaks consistent with a single $Co_3V_2O_8$ structure (Fig. S3). Specifically, as shown in the expanded XRD patterns, crystallization increased as the annealing time increased; in other words, the longer the sample went through the calcination process at 500 °C, the higher crystallinity.

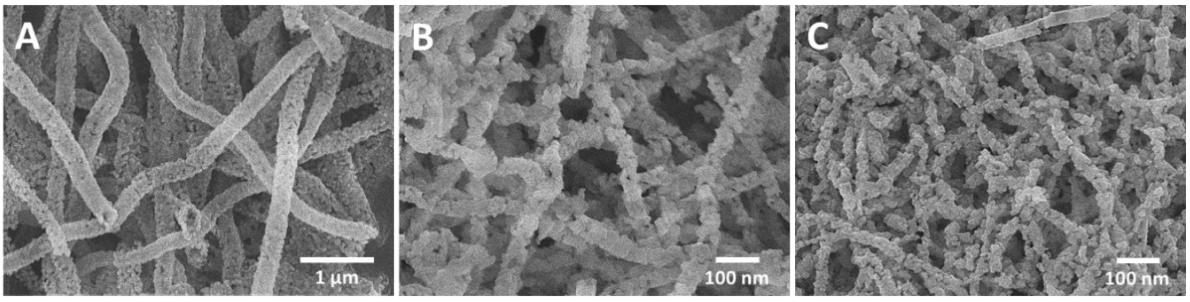

Fig. S4. SEM images of Co/V mixed oxides after being thermally calcined for 1 h at various annealing temperatures of (A) 500 °C, (B) 650 °C and (C) 800 °C, respectively. Note that prepared samples (A-C) are consistent with the samples (A-C) in Fig. S2.

Shape and morphology of as-prepared Co/V mixed oxides at different annealing temperatures (Fig. S4) and retention times (Fig. S5) were examined by SEM. As shown in Fig. S4, it is clear that the nanosturcutres prepared at relatively low temperature (500 °C) have highly porous nanofibrous shape. However, as the annealing temperature increased (~800 °C), the post-calcined nanostructures lost the fiber structure and formed the aggregation when compared to the sample at 500 °C. Depending on the annealing conditions, morphological features of the samples changed rapidly not only according to the temperature but also the retetntion time (Fig. S5). It was observed that the diameter of the nanofiber became decrease in the following order: (A) > (B) > (C). That is, as the retention time increased, size of the fibrous nanostructure was shrunk and the structural integrity was decreased with 180-min retention. Therefore, retention time under the calcination process is an important parameter to tune the morphology of nanofiber as well as the annealing temperature. In conclusion, the calcination at 500 °C for 60 min was optimal to fabricate a nanotubular structure composed of mainly $Co_3V_2O_8$.

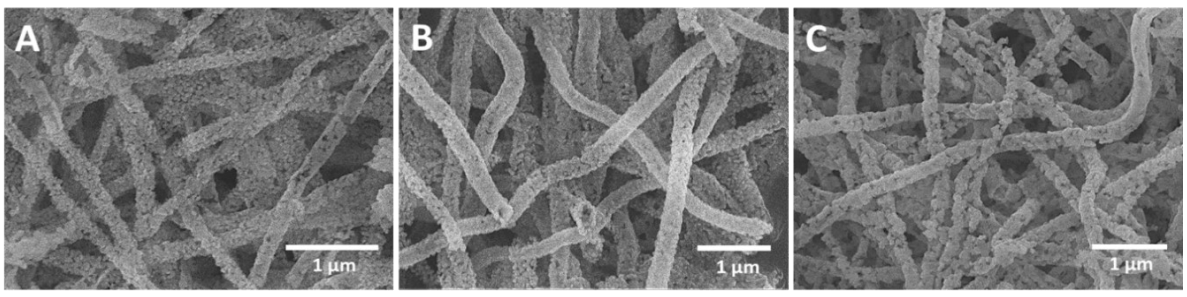

Fig. S5. SEM images of Co/V mixed oxides after being thermally annealed at 500 °C with (A-C) different retention times: (A) 20 min, (B) 60 min and (C) 180 min. Note that prepared samples (A-C) are consistent with the samples (A-C) in Fig. S3.

Table S1. Comparison of the analytical performances of $Co_3V_2O_8$ nanofibers with other catalysts reported previously for AA sensing.

Sample	Method	Solution	Sensitivity ($\mu A\ mM^{-1}\ cm^{-2}$)	Linear range (μM)	Reference
$Co_3V_2O_8$ nanofibers	*Amp	0.1 M PBS (pH 7.4)	82.16	20-500	This work
C_3F_7-azo$^+$/RGO	**DPV	0.1 M PBS (pH= 8.0)	***42.59	57.3–134.3	*Talanta,* 2022, **237**, 122986
$CdO/SnO_2/V_2O_5$ micro-sheets (MSs)	Amp	PBS (pH 7.0)	21.34	0.0001-10	*SN Appl. Sci.*, 2020, **2**, 1953
GCE/GNP-coPIL_1@$Fe(CN)_6^{3-}$	Amp	PBS (pH 7.0)	***0.08	25-300	*J. Phys. Chem. C.* 2019, **123**, 19637–19648
AC-RuON-GCE	DPV	PBS (pH 7.0)	85.9	47–181.8	*Electrochem. Commun*. 2000, **2**, 90–93
Screen-printing RuO_2	Amp	PBS (pH 7.4)	2.79	0–4000	*Int. J. Electrochem. Sci*. 2011, **6**, 2688–2709
H-rGO/GCE	DPV	B-R buffer solution (pH 6.0)	385.0	1-100	*Sens. Actuators B: Chem*., 2015, **207**, 535-541
Ni/Ag@rGO	DPV	0.2 M PBS (pH 7.0)	23.3818	4.89–90.09	*J. Alloy Comp.,* 2020. **842**, 155873
RuO_2/Au	Amp	0.1 M PBS (pH 7.4)	377.8	20-1000	*Sens. Actuators B: Chem*., 2018, **255**, 316–324
RuO_2 NRs-WO_3 NFs	Amp	PBS (pH 7.4)	171.7	5–2000	*Sensors*, 2019, **19**, 3295

*Amp, amperometry; **DPV, differential pulse voltammetry; ***The unit of sensitivity is $\mu A\ mM^{-1}$.